Pergamon

Int. J. Solids Structures Vol. 35, No. 19, pp. 2487–2503, 1998
© 1998 Elsevier Science Ltd
All rights reserved. Printed in Great Britain
0020–7683/98 $19.00 + .00

PII: S0020–7683(97)00146–7

INTRINSIC FAILURE MODES OF BRITTLE MATERIALS

D. KRAJCINOVIC and M. VUJOSEVIC†
Mechanical and Aerospace Engineering, Arizona State University, Tempe, AZ, U.S.A.

(*Received* 19 *May* 1997)

Abstract—The present study reviews the application of damage mechanics to the prediction of the material failure caused by the evolving density of microcracks. The loss of homogeneity on the specimen size is common to all failure modes considered in this study. The transition between a statistically homogeneous to a heterogeneous state of strain and damage depends on the morphology of defect clusters, state of stress, strain rate and microstructural disorder. As a result the failure can occur in several different ways. A rich spectrum of physical phenomena and new concepts that emerge from these considerations demonstrates the successes and limitations of the traditional, deterministic, and local continuum models. © 1998 Elsevier Science Ltd. All rights reserved.

1. INTRODUCTION

The narrow objective of this study is to provide an overview of a class of failure modes and shed some light on the effect that the damage has on the material failures and provide and discuss the role of damage mechanics in the analyses of material failures. The discussion is limited to the failure modes attributed to the critical values of effective material parameters. The study is further limited to the materials with a relatively modest cohesive strength that exhibit a strong disposition to microcracking. Non-crystalline rocks, concrete, glass, ceramics, silicon, human bones, iron and most thermosets belong to this class of materials. Finally, the discussion focuses on the crack-like defects with an atomically sharp tip giving rise to large stress concentrations. Conceptually, if not always directly, most of the discussion within this study is also pertinent to the materials replete with voids.

2. MATERIAL CHARACTERIZATION

With the recent advent of micromechanics "the doctrine that *all* observable events must be explained as macro events; that is to say, as averages or summations of certain micro events" (Popper, 1980) is widely believed to be true. However, the validity of this "doctrine" may become debatable if the disorder on a finer scale affects the response on the coarse scale in a manner that is not related to "averages or summations". More precisely, the averages provide a meaningful macro-representation of the micro-events only if a set of precisely defined conditions is satisfied.

The microstructure of an overwhelming fraction of engineering materials is geometrically, topologically and chemically (structurally) disordered. A complete statistical description of the microstructural disorder (including a variety of micro defects) is never available and, perhaps, only seldom required. Nevertheless, the introduction of few characteristic lengths, which qualitatively and quantitatively define the major features of the disorder, often suffice to examine the validity of assumptions and simplifications on which some of the continuum and micromechanical failure models are based.

For computational efficiency a system is often subdivided into sub-systems (say, finite elements). The "effective" material properties of the sub-system (or a material point in continuum models) are determined from the orientation weighted volume averages of different phases (inclusions) and micro-defects applying one of the mean field methods of

† Current address: Technology and Product Development, Sensor Products Division, Motorola, Phoenix, AZ, U.S.A.

micromechanics (Mura, 1982; Nemat-Nasser and Hori, 1993; Krajcinovic, 1996). The main assumption on which these models are based is that the material is *translationally invariant*, i.e. that the exact locations of each inclusion and micro-defect within a sub-system have no effect on the macroscopic response. Thus, the traditional mean field, local models of mechanics are applicable if and only if the material and its response are statistically homogeneous on a "small enough" scale.

A volume of a given material and its response are statistically homogeneous or translationally invariant (Krajcinovic, 1996) if the inequalities

$$\max(L_m, \xi) < L_{rve} < L \quad \text{and} \quad \left|\frac{\partial \sigma^0}{\partial x}\right| L_{rve} \ll |\sigma^0| \tag{1}$$

are satisfied. In (1) σ^0 is the average stress imparted to the external surfaces of the volume, while L and L_m are the characteristic lengths of the specimen and material texture (such as the grain size in granular materials and internodular distance in resins). Finally, ξ is the largest length over which the defects are correlated and L_{rve} the characteristic length of the representative volume element (RVE) defined as the smallest volume for which the conditions (1) are satisfied (Nemat-Nasser and Hori, 1993; Ostoja-Starzewski, 1994; Krajcinovic, 1996). Two or more defects are considered to be correlated, and form a *cluster*, if their growth depends on their interaction. Hence, the correlation length is proportional to the size of the largest cluster. Naturally, sub-systems (such as finite elements) must be larger than the RVE.

In the case when the condition (1a) is satisfied the effective properties of the volume depend on the density of active defects (including their orientation) and are independent of the precise locations and individual sizes of heterogeneities and defects. If the second inequality in (1) is not satisfied the exact position of a defect is important due to the fact that the stress is not homogeneous. This condition governs the size of RVE in the case of rapidly changing stresses in the vicinity of a macrocrack tip or notch.

3. DAMAGE AND DAMAGE EVOLUTION

A crack is considered to be a *microcrack* if it is commensurate to the characteristic length of the material microstructure L_m. A microcrack can be either *active* or *passive* depending on whether they support a discontinuity in the local displacement field or not. For a *given state* of stress only the active cracks affect the effective material parameters and macroscopic response. Hence, the *damage* can be measured by the effect that the active micro-defects have on the effective material (transfer) properties. The *damage evolution* is a non-equilibrium, irreversible thermodynamic process during which the total number of bonds in the material decreases and the total area of internal surfaces is increased.

Owing to the translational invariance an ensemble of microcracks can affect the effective properties of a statistically homogeneous volume only through their density function pictorially represented by the rosette histogram (Krajcinovic, 1996). Since the direct measurements of the radii, shapes and orientation of each crack in a volume are not possible the damage in a statistically homogeneous volume can be measured indirectly by the effect it has on the stiffness tensor.

Damage evolution is a macroscopic manifestation of the net loss of interatomic bonds in the course of the nucleation of new and growth of the existing microcracks. A microcrack will nucleate if the local tensile or shear stress exceeds the local nucleation strength of the material, i.e. if $\sigma(x_0) \geqslant \sigma_{nuc}(x_0)$.

An existing crack will start propagating when the elastic energy release rate G stored in the vicinity of its tip exceeds the thermodynamic force R resisting its growth, i.e. when

$$G[\sigma(x)] \geqslant R(x). \tag{2}$$

The energy release rate G depends on the elastic energy and potential energy of applied

forces. A crack can grow only if at least one of the three stress intensity factors is positive. When all three stress intensity factors are negative a crack is dormant (does not grow) and almost always *passive* since it does not affect local deformations and effective parameters.

The exact determination of the thermodynamic force G is a difficult proposition since the microcracks are of irregular shapes, seldom planar, often interfacial and embedded in a material that is neither isotropic nor homogeneous on the considered scale. The stress to which the microcracks are subjected may also be altered by the interaction with the adjacent microcracks and/or stress concentrations at the heterogeneities. The resisting force R (cohesive or fracture energy) depends on the spatial distribution of energy barriers (grain boundaries, particle of fiber reinforcement, etc.) that are strong enough to prevent or hinder the propagation of a microcrack. Thermodynamic forces G and R also depend on the accumulated damage. In summary, the spatial distributions of G and R are random functions of coordinates in a material with a random microstructure.

The statistical aspect of the crack nucleation is related to the fact that the spatial distribution of nucleation sites is random. The onset of crack propagation depends on the stochastic function $\{G[\sigma(x)]/R(x)\}$ and, therefore, on the microstructural disorder. Damage evolution mode is influenced by the stress concentration at microstructural heterogeneities (hot spots, large σ or G) and internal surfaces of inferior cohesive (fracture) strength (weak links, small σ_{nuc} or R). Stress distribution is, at larger damage concentrations, multifractal (Hansen and Roux, 1988; Krajcinovic, 1996). A material is *damage tolerant* if its microstructure is micro-heterogeneous, i.e. if the band-width of the distribution of thermodynamic forces $R(x)$ is wide enough to arrest growing cracks. Hence, the damage can evolve in heterogeneous materials (such as composites) by both crack nucleation and stable growth of cracks. In contrast, microcrack growth in *damage sensitive* materials [with a homogeneous microstructure characterized by a narrow band-width of the distribution of $R(x)$] subjected to uniform tensile stresses is typically unstable. The probability density function (pdf) of the force $R(x_0)$ in the material point x_0 of a damage tolerant and damage sensitive solid are sketched symbolically in Fig. 1.

The damage evolution in damage tolerant materials is, at least initially, controlled by a random nucleation of microcracks. In the absence of initial defects the stress concentrations are few and the band-width of the pdf of $G[\sigma(x_0)]$ is narrow. As the number of defects multiplies the stress concentrations become more frequent, the band-width of the pdf of $G[\sigma(x_0)]$ widens (Fig. 2) and the probability that $\{G[\sigma(x_0)]/R(x_0)\} = 1$ in x_0 increases. The depletion of weak spots makes the crack nucleation at large damage concentration less probable. Hence, the balance tilts from the defect nucleation to defect growth. The state of damage at which the cross-over from microcrack nucleation to a microcrack growth damage evolution takes place depends, therefore, on the spatial dispersion of material points in which the ratio $\{G[\sigma(x)]/R(x)\}$ exceeds unity.

In summary, the intrinsic brittle to quasi-brittle transition depends on the size of existing defects and the band-width of the distribution of the thermodynamic force $R(x)$ which characterizes the microstructural disorder and capacity of a brittle material to dissipate the imparted energy before it fractures on the macroscopic scale (Roux and

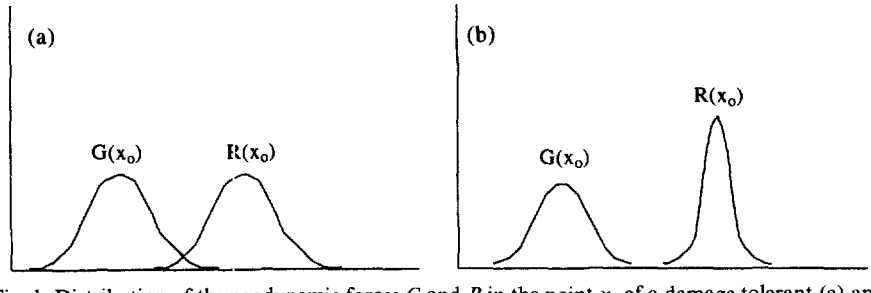

Fig. 1. Distribution of thermodynamic forces G and R in the point x_0 of a damage tolerant (a) and a damage sensitive solid (b).

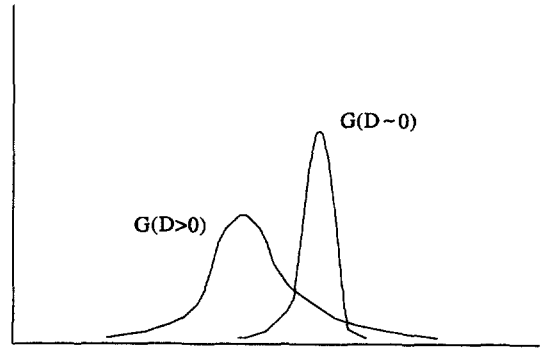

Fig. 2. Change of the band-width of the distribution of the thermodynamic force G in the point x_0 related to the accumulating damage D.

Hansen, 1990; Hansen and Roux, 1991; Krajcinovic, 1996). The traditional, phenomenological and deterministic definition of the brittle to quasi-brittle transition (Paterson, 1978), based on macroscopic observations, is strongly dependent on the specimen size and shape and is, therefore, not always a material (intensive) parameter.

4. INTRINSIC FAILURE MODES

A failure is *intrinsic* if its onset is related to a critical value of an effective (intensive) material property. Consistent to the proposed measure of damage, the onset of an intrinsic failure mode must be a function of the volume averages of stresses and damage. Hence, a failure is intrinsic only when the material and response in the state precursory to the failure threshold is either statistically homogeneous or statistically self-similar. The present study will address several different cases of intrinsic failures of materials susceptible to microcracking when subjected to the long range compressive stresses.

This study will review and synthesize three different modes of intrinsic failures:

(a) strain localization during which only the microcracks within a narrow band grow;
(b) percolation during which microcracks do not grow at all;
(c) creep rupture attributed to random fluctuations of temperature.

The above listed failure modes are chosen due to their intrinsic importance and the fact that they have several aspects in common. At the same time the rate at which the correlation length increases in these three processes is different due to the size of the volume within which the energy available for cracking is stored. The rate of softening depends on the rate at which the correlation length increases, i.e. on the volume within which the excess energy $(G-R)$ is stored. The slope of the "softening" part of the force–deformation curve is steepest in the case of a single propagating crack since the correlation length (its length) increases at a rate of 0.4 of Rayleigh waves and minimum in percolation when the cluster grows rather slowly. The slope of the softening part of the force–deformation curve during strain localization is not quite as steep, since the excess energy is stored along the entire fault perimeter.

Finite element analyses of the growth of defect clusters in disordered materials are prohibitive in view of necessary re-meshing and formation of a representative statistical sample. Limiting the scope to qualitative analyses two-dimensional lattices of modest sizes proved to be very valuable in estimating the effect of the disorder on the onset of failure and post-failure response.

4.1. *Strain localization*

In a typical, deformation controlled, strain localization test [see Hallbauer *et al.* (1973); Lockner *et al.* (1992)] a brittle (rock or concrete) cylindrical specimen is initially subjected to a hydrostatic compression to which is, subsequently, superimposed a quasi-statically incremented contraction in the axial direction. Phenomenologically, the specimen passes

bias of the stress amplifying effect of crack interaction. The propagation of clusters is attributed to the *cooperative effect*, i.e. the interaction driven growth of constituent cracks.

At a critical damage concentration one of the cluster (nascent fault) becomes dominant and the specimen ceases to be homogeneous when the correlation length ξ approaches the specimen size L. The loss of homogeneity is caused by large difference between the effective parameters (damage density) of the materials in the interior and exterior of the fault. The material in the fault interior is strongly heterogeneous, while the exterior volume relaxes elastically and remains homogeneous. The nascent fault grows in the *avalanche* mode since the disordering aspect of the crack growth increases at the expense of the ordering (mean field) effect of the crack nucleation.

A majority of the *continuum* mechanics models view the strain localization as being the quasi-static Hadamard's instability (bifurcation) of the material constitutive description (Rudnicki and Rice, 1975; Rice, 1976). Assuming that the material is statistically homogeneous at the state of incipient bifurcation the onset of localization and the fault orientation are determined from the condition.

$$\det\|\mathbf{n}\cdot\bar{\mathbf{C}}_t\cdot\mathbf{n}\| = \det\|\mathbf{Q}\| = 0 \tag{3}$$

where $\mathbf{Q}$ and $\bar{\mathbf{C}}_t$ are the effective acoustic and effective tangential stiffness (elasticity) tensors, while $\mathbf{n}$ is the normal to the fault perimeter.

The simplicity, elegance and mathematical clarity of Rudnicki and Rice (1975) model and condition (3) inspired an interest into the localization failure which is still not abating. However, the simplicity is often replete with limitations and the models based on condition (3) were not an exception to this rule. Local, quasi-static continuum models of faulting predict that a zero-volume fault forms instantaneously across the entire specimen. These predictions of fault kinematics were refuted by the experimental data (Hallbauer *et al.*, 1973; Lockner *et al.*, 1992; Reches and Lockner, 1994) and particle dynamic simulations (Krajcinovic and Vujosevic, 1998). The strong dependence of the condition (3) on the details of the constitutive law (Rice, 1976) was another indication that a rational model must incorporate the statistical aspects of the material and disorder (accumulated damage).

The effect of the dynamic nature of the strain localization and disorder on the specimen response at the localization transition were the primary inducements for the application of the particle dynamics model (Krajcinovic and Vujosevic, 1998). The mass of the solid is lumped into 3535 particles (nodes), connected to their nearest neighbors by central-force Hookean links of equal stiffness, and forming a two-dimensional triangular lattice. The spring rupture strengths was taken to be infinite in compression, while the tensile strengths f_{ci} were distributed uniformly, i.e. $p(f_{ci}) = \text{const}$. Model induced orientations of the lattice were minimized by adopting a normal distribution of link lengths.

To match Lockner *et al.* (1992) specimens the aspect ratio of the lattice is taken to be equal to 2.5. The loading was also selected to match these tests by subjecting the lattice first to the biaxial (hydrostatic) compression and, subsequently, to quasi-static and monotonic contraction in the axial direction. A link was removed when the force it transmits reached it tensile strength $f_i = f_{ci}$. The next increment was applied only when the kinetic energy of the lattice fell below a very small level. A minimum of damping was introduced within the framework of Varlet algorithm to remove the kinetic energy in each loading step.

Particle dynamics simulations confirmed that the deformation is initially homogeneous [Fig. 3(a)] prior to the formation of several small faults just ahead of the peak of the force-contraction curve [Fig. 3(b)]. At the peak one of the bands (fault) grows rapidly, but not instantaneously, across the specimen at the angle suggested by the continuum models. The compliance of the fault (along its length) is many times larger than the compliance of the rest of the specimen. Thus, in the deformation controlled conditions the stresses in the exterior of the fault must relax and the strain concentration in all other shear bands is almost entirely eliminated [Fig. 3(c)].

The actual band that will develop into a fault cannot be determined *a priori* since it depends on the lattice disorder. It is also difficult to pinpoint the exact state at which the material ceases to be statistically homogeneous on the specimen scale as $\xi \to L$. However, it is certain that the strain field within the softening regime is not homogeneous. Once the

specimen ceases to be homogeneous the volume averaging becomes meaningless and the only meaningful relation is that between the resultant force and system elongation. The division of the specimen into sub-systems becomes coarser as ξ grows. In the aftermath of the localization transition the localized band cannot be sub-divided since $\xi \approx L$.

The simulations were limited to two-dimensional lattices by the available computational capacity. In the absence of micromechanical data (stiffness and strength of the adhesion between individual grains of granite) it was not possible to match the test data details quantitatively. Nevertheless, the simulations data qualitatively matched all salient aspects of the faulting recorded in tests. According to lattice simulations the band orientation was, indeed, found to be 34° while the macro response and patterns of damage evolution closely match (Fig. 4) the experimental (acoustic emissions) data in Lockner *et al.* (1992).

Problems related to the damage modeling are illuminated by Fig. 5. The accumulated damage (fraction of broken bonds) is initially a linear function of strains. However, near the peak of stress–strain curve the fraction of broken bonds doubles almost instantaneously. The plateau reached by the axial strain and damage density within the post-softening regime is attributed to the fact that the lattice shear stress ($\sigma_{ax} - \sigma_{lat}$) decreases below the frictional (or interlock) resistance to sliding within the fault.

At the peak of the force-contraction curve only 6.25% of the links were ruptured. To test whether the localization onset critically depends on the details of constitutive relations (Rice, 1976) the "material" is "embrittled" by narrowing the band-width of the link strength by 25% (decreasing the difference between the strengths of the weakest and strongest links from unity to 0.75). Indeed, the fraction of ruptured links at the peak of the stress–strain curve was reduced (by a factor of 3) to 2.1%. In the limit, fault formation in a perfectly periodic brittle lattice (all links of equal length, strength and stiffness) requires only 0.3% of ruptured links [Fig. 6(a)]. Twice as many links must be ruptured to cleave a perfect triangular lattice in uniaxial tension by a macrocrack propagating through a single row of links [Fig. 6(b)].

In summary, the energy required to break the links prior to the onset of softening regime depends to a large extent on the band-width of the links strength (damage tolerance) and is always larger than the energy needed for the brittle fracture of a damage sensitive specimen subjected to the tensile and/or shear tractions. Even a modest level of disorder suffices to increase the energy needed for the localization failure through the evolution of the diffused damage. The sensitivity of condition (3) to the details of microstructural fabric is a serious modeling challenge. As the dominant role in damage evolution shifts from the crack nucleation to interaction and clustering of cracks the governing statistics crosses over from the averages to extreme moments of stress and damage distribution. A realistic analytical description of this complex process must incorporate the dominant role of the damage and cooperative effect on the localization onset.

The determination of the fault width, often considered to be a material constant, is an interesting but non-trivial exercise. Since the cracks of the fault do not intersect and since the degree of correlation is not a yes-or-no proposition, the question whether a nearby crack is a part of the fault does not have a definitive and unambiguous answer. In the language of statistics the fault volume is not a purely geometrical concept since the distances between the adjacent cracks are continuously distributed and the crossover length separating correlated and non-correlating cracks depends on the crack shapes, sizes, orientations, local state of stress, effective parameters of the specimen, etc. Any deterministic prediction of this length is, therefore, largely arbitrary. Since the geometry of the fault is very irregular and its width is not constant (Fig. 4) the estimate of the proper fault "width" depends on the resolution, observer and observation scale. However, by definition, the fault "width" must be always a multiple of the characteristic texture length L_m as claimed by Bazant and Cedolin (1991) for concrete and rocks and Vardoulakis and Graf (1985) for sand. Furthermore, Sornette *et al.* (1990) determined the fault length as $L_f \propto L^{D_f}$. Unfortunately, the fractal exponent $D_f = 1.70 \pm 0.05$ was determined assuming that the propagation of the cluster is dominated by the diffusion-limited aggregation rather than stress concentrations (cooperative effect).

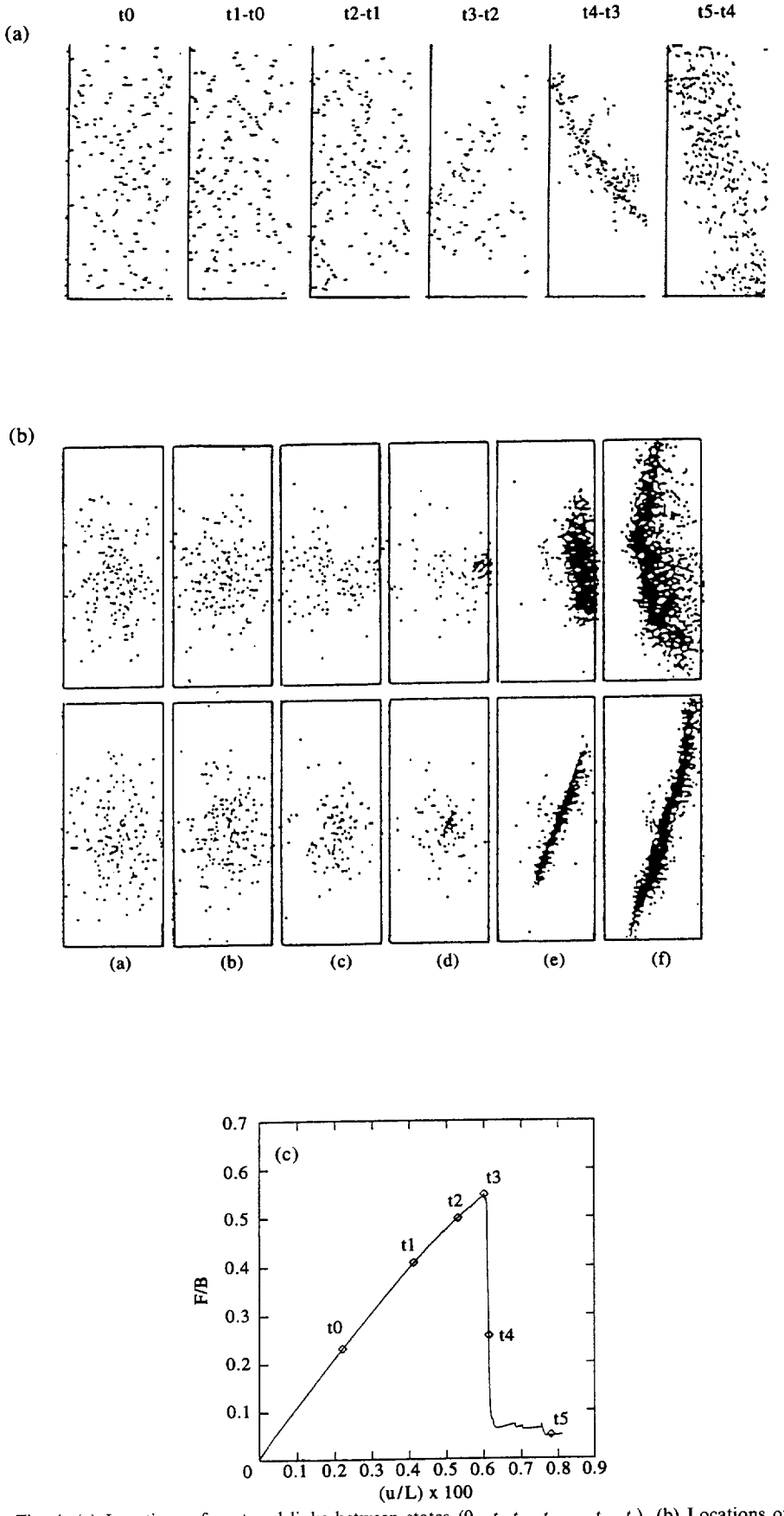

Fig. 4. (a) Locations of ruptured links between states $(0-t_0, t_0-t_1, \ldots, t_4-t_5)$, (b) Locations of acoustic emissions reported in Lockner *et al.* (1992) and (c) force–contraction curve.

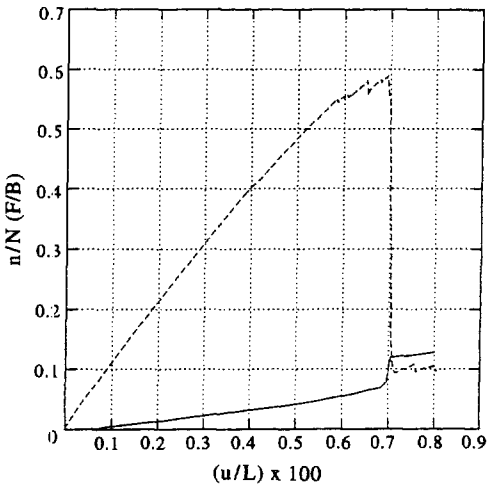

Fig. 5. Force contraction (dotted line) and fraction of ruptured links (solid line) plotted vs the specimen strain.

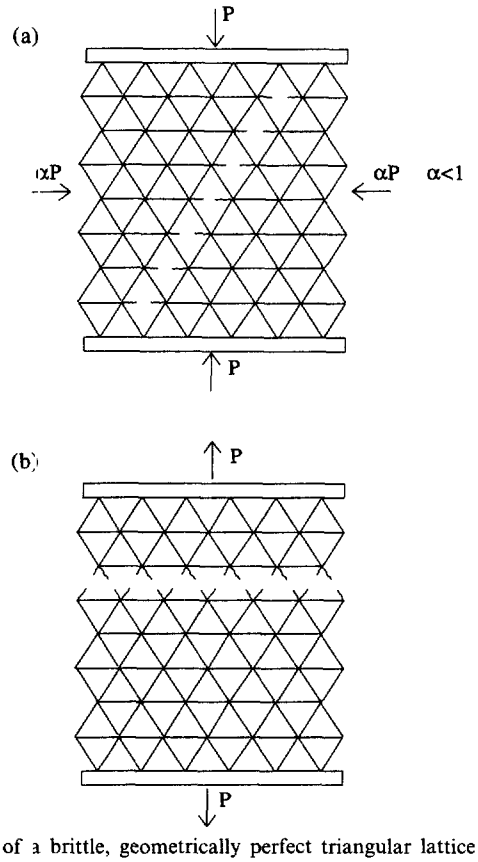

Fig. 6. Failure modes of a brittle, geometrically perfect triangular lattice in: (a) shear and (b) cleavage.

Recalling that the damage is defined by the effect that microcracks have on the effective properties it is reasonable to measure the fault "width" accordingly. The considered effective property of the system must reflect two principal aspects of the strain localization process; disorder and dynamics of the fault growth. Starting from this premise Krajcinovic and Vujosevic (preprint) measured the fault "width" indirectly by considering the transfer of elastic energy through the faulted specimen. The distance through which an elastic wave

cluster separates the specimen into two parts. Thus, the conditions defining the onset of percolation is

$$\xi \to L \quad \text{as} f \to f_{ce} \tag{5}$$

where f and f_{ce} are the density and critical density of randomly inserted voids or cracks.

The effective stiffness measured in the percolation tests is actually the secant stiffness (Krajcinovic, 1996) since the damage remains constant during the process of the stiffness measurement. The path along which the stiffness is measured during a percolation test corresponds to the unloading from a state of a deformation process during which the same defect distribution is realized by the nucleation only (Krajcinovic, 1996).

The density of defects at the elastic percolation transition depends on the topology of the system and defect geometry. Three aspects of the percolation test are of crucial importance: (a) the defects are randomly distributed throughout the system; (b) the existing defects are not allowed to grow; and (c) the thermodynamic force G has no effect on the damage evolution. Nevertheless, the described topological exercise has a mechanical meaning. Since the spatial distribution of defects is random and the defects do not grow as a result of the excess energy, a percolation process corresponds to the damage evolution that is driven *exclusively* by the defect nucleation. The described conditions are typical of the case when cracks are subjected to the compressive normal stresses and negligible shear stresses (such that the SIFs of all cracks are negative). These conditions can be realized only in the limit of the infinite damage tolerance since the damage evolution is independent of the stress concentrations.

The damage induced by a perfectly random nucleation of defects is, by definition, isotropic. Manipulating the derivations in Garboczi and Thorpe (1985) the self-consistent estimates of the components of the stiffness (elastic) tensor of a central-force elastic lattice can be written in the form

$$\bar{C}_{ijmn} = C^0_{ijmn}(1-D) \quad \text{where} \quad D = q/q_{ce} \tag{6}$$

typical of damage mechanics models. In (6) the superscript "0" stands for pristine lattice $D = 0$, q for the fraction of ruptured links and q_{ce} for the elastic percolation threshold which depends only on the lattice geometry. Using the methods of continuum percolation the expressions identical to (6) were derived for the elastic plate weakened by voids (Xia and Thorpe, 1988; Krajcinovic *et al.*, 1992; Krajcinovic, 1996) and rectilinear slits (Krajcinovic *et al.* 1992b). The parameter D is equal to the porosity (in the case of voids) and to Budiansky–O'Connell parameter (in the case of slits). Finally, the isotropic (scalar) continuum models (Lemaitre, 1992) are based on relation (6).

Nominally, the expression (6) for the effective stiffness is applicable only in the limit of a dilute concentration of defects, i.e. $\xi \ll L$. As $\xi \to L$ the largest defect cluster percolates through the system disconnecting it into two large fragments. In the neighborhood of percolation threshold ($\xi \to L^-$), the homogeneity is lost on the scale of the specimen and in the absence of any other scale the geometry of specimen becomes self similar (scale invariant). Hence, the geometry of the largest defect is fractal in the limit of the infinitely large specimen $L \to \infty$. The stress field in the neighborhood of the percolation threshold cannot be described by the volume averages only. The microstructural disorder and the attendant stress fluctuations are largest near the percolation threshold.

The self-consistent estimates of the percolation transition are very accurate except for the case of overlapping (intersecting) defects (Krajcinovic, 1996). The scaling law for the effective secant modulus $\bar{C}_{sec}$ of the system reduces near the percolation transition is

$$\bar{C}_{sec} \propto (f-f_{ce})^r \quad \text{as} f \to f_{ce} \tag{7}$$

where f is the damage density, r a universal exponent that depends on the defect shape and orientation and on whether the defects are allowed to overlap or not. Since the exponent r

is usually larger than one the rate at which the effective secant stiffness changes near the percolation transition $f \to f_{ce}$ is very slow. The scaling law (8) for the effective secant stiffness cannot be predicted with any accuracy from the mean field model. For example, according to the self-consistent micromechanical damage model of type (6) $r = 1$.

Simulations and finite elements computations indicate that the linear relation between the damage and effective stiffness (6) is in the case of the random nucleation of defects accurate until the stiffness is reduced to approximately 15% of its original value (Jasiuk *et al.*, 1994). The damage evolution in the crossover region, connecting self-consistent regime (in which the local damage models are applicable) and the percolation regime (within which the damage can be determined by mean field micromechanical models), is driven by the interaction of large defect clusters. Nonlinear damage modes suitable for the analyses within the crossover regime have as yet to be formulated.

It is interesting to note that the elastic energy of vibrations is also localized in the asymptotic neighborhood of the percolation threshold. Perturbations (fractions) excited within the defect cluster do not spread over the entire sample. The decay length L_w of periodic perturbations with frequency ω in a percolating lattice scales as

$$L_w(\omega) \propto \omega^{-2k'} \tag{8}$$

where $k' \approx 0.35$ and 0.27 (Stauffer and Aharoni, 1992) in two and three dimensions, respectively. In analogy to the strain localization (4) the decay length tends to infinity (and the density of states or vibrational modes becomes zero) in the static limit (i.e. when the perturbation frequency approaches zero).

The described damage evolution mode is typical of specimens subjected to the hydrostatic compression, high velocity impact (Mastilovic *et al.* 1996), comminution (crushing), creep at small stresses and large temperatures (Vujosevic and Krajcinovic, 1997). It also takes place during the process of solidification (curing) (Krajcinovic and Mallick, 1995) or corrosion (Gaudett and Scully, 1994), loss of stiffness in network glasses (Cai and Thorpe, 1989), etc. Finally, the percolation models can be used to select the most accurate mean-field model. They also prove that in balance the interaction of randomly distributed defects has, in contradiction to the mean-field micro-mechanical models (Horii and Sahasakmontri, 1990; Ju and Tseng, 1995), a shielding effect.

4.3. *Creep rupture of polymers*

A material exposed to a high temperature environment may fail even when the stresses are well below its mechanical strength. This failure mode, known as the creep rupture, is of substantial importance in design. A variety of empirical, phenomenological (Hult, 1974) and micromechanical (Riedel, 1987) models were proposed to predict the time to creep failure as a function of the temperature and applied stress. A majority of mechanics models are not only deterministic but are based on the assumption that the influence of the temperature on the system response and failure can be introduced by adjusting the constitutive description of the material. Material science models (Regel' *et al.*, 1974) treat the temperature as the basic stimulus that enhances the atom mobility and intensifies the mobility of dislocation motion (ductile slip) and rate of rupture of atomic bonds (damage evolution).

The nano-structure of epoxy resins, that consists of a set of dense nodules interconnected by links of lower density (Krajcinovic and Mallick, 1995), resembles a three-dimensional lattice. The stochastic nature of the damage evolution in the lattice, related to the spatially and temporally random fluctuations of the temperatures, can be introduced using the absolute reaction-rate theory of Eyring (1936) [see also Termonia *et al.* (1985)]. According to this theory the kinetics of the damage evolution (bond ruptures) is related to the probability that the kinetic energy supplied by the temperature fluctuations and strain energy will exceed the energy needed to dissociate two adjacent atoms. The probability that the ith lattice link will rupture during the time interval Δt is (Vujosevic and Krajcinovic, 1997)

$$p_i = \frac{1}{t_0}\exp\left[-\frac{U_0-(f_i^2/2k)}{k_b T}\right]\Delta t \tag{9}$$

where f_i is the force transmitted by the link of stiffness k, while t_0, T, U_0 and k_b are the period of the free vibration of an atom, temperature (in degrees of Kelvin), apparent activation energy and Boltzmann constant. Relation between conditions (9) and (2) is discussed by Krausz and Krausz (1988), Lawn (1993) and Krajcinovic (1996). The link stiffness k can be estimated from the morphology of the network of constituent molecular chains (Krajcinovic and Mallick, 1995).

The resin nano-structure is in Vujosevic and Krajcinovic (1997) model approximated by a two-dimensional triangular central-force lattice which was in its pristine state ordered, i.e. all links were of equal length, strength and stiffness. Enforcing periodic boundary conditions along its vertical edges the lattice is rendered infinite in the horizontal direction and the effect of the specimen shape is eliminated. The simulations were performed for lattices of five different sizes (λ = 12, 16, 20, 24, 32, where λ is the number of link rows in the vertical direction) and three different values of the load parameter $\alpha = (f_i^2/2kU)|_0$ (α = 0.001, 0.01 and 0.03, see Figs 7, 8). The subscript "0" refers to the pristine state of the system.

The average temperature was kept fixed at 0.75 of the homologous temperature and stationary tensile tractions were applied to a rigid bar on the top end in the vertical direction while the bottom end was hinged to a rigid foundation. Link forces f_i were computed using truss analyses and the sequence of link ruptures was determined by Monte-Carlo lottery in conjunction with the stochastic rupture conditions (9). Hence, the disorder is attributed to the random fluctuations of temperature rather than being frozen (quenched) into the lattice.

The time to failure depends strongly on the load parameter α and weakly on the specimen size (Fig. 8). The progressive loss of the axial stiffness is also depicted in Fig. 8. Damage evolution is in the case of negligible tensile stresses driven by the random fluctuations of the temperature and is similar to that described in the case of percolation. In the limit of vanishing α the damage at the creep rupture tends to the percolation limit (6) of $q_{ce} \approx 0.35$ (where q_{ce} is the fraction of ruptured bonds at the percolation transition). The increase of the strain rate in the tertiary phase, manifested by the precipitous decline of lattice stiffness (Fig. 8), is related to the formation of a large defect cluster and attendant stress concentration.

Simulation results are plotted on the left side while the results of a simple analytical model are shown on the right side of Fig. 9. This one-parameter model is based on the

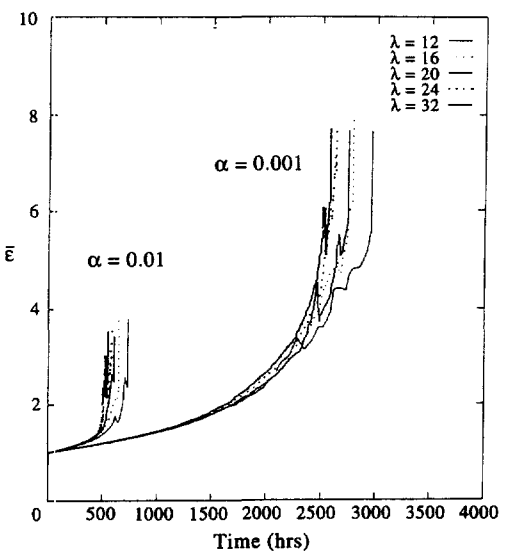

Fig. 7. Creep strain plotted vs time for two values of the load ratio α.

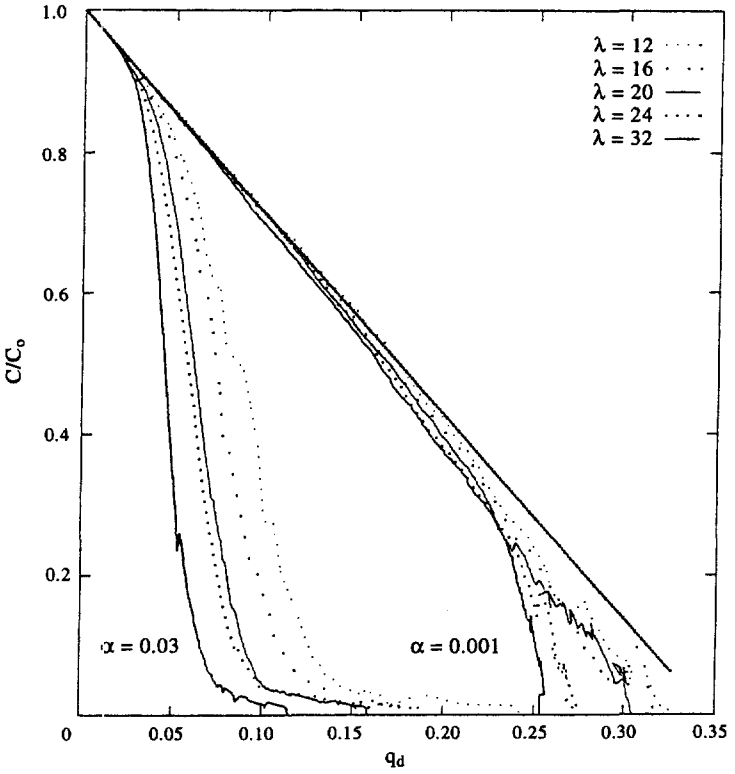

Fig. 8. The normalized effective axial stiffness of the lattice plotted vs the fraction of ruptured links for two values of the load ratio α.

damage parameter $D(t) = [C^0 - C(t)]/C^0$ identical to (6b). The relation between the rates of strain and damage are derived from the Tobolsky–Eyring model [according to which the strain is proportional to the logarithm of the elapsed time, Vujosevic and Krajcinovic (1997)]. The final form of this simple (but nonlinear) uniaxial damage model

$$\frac{\varepsilon(t)}{\varepsilon_e} = 1 + \frac{1}{q_{ce} t_0} \exp\left[-\frac{U_0(1-\alpha)}{k_b T}\right] t_f \ln\left(\frac{t_f}{t_f - t}\right) \tag{10}$$

fits the simulation curve (along its entire length) in a very satisfactory fashion (Fig. 9). An even simpler mean field model (that neglects the stress concentrations caused by the accumulated damage) provides only an upper bound on the time to failure that exceeded the simulation data by a factor of eight for the largest value of parameter α. Hence, the damage accumulation driven by the stress concentrations cannot be neglected in the predictions of the response within the tertiary creep and time to failure.

The lattice model of a resin is morphologically correct only on the molecular (nodule) scale. However, the simulations in Vujosevic and Krajcinovic (1997) show that the time to failure depends on the specimen size only if $L \leqslant 0.5$ μm. The independence on the scale, corroborated by the test data in Regel' *et al.* (1974), is related to the weak effect of the specimen size on the crack nucleation events. Hence, the size independence of the time to failure becomes an issue only for the pre-damaged specimens and when the applied stress is a dominant cause of the damage evolution.

5. SUMMARY AND CONCLUSIONS

This review was prompted by a frequently held opinion that the damage parameter is not correlated to the specimen strength and that the damage mechanics models cannot be used to estimate the failure threshold. While only partially true, this opinion is generalized

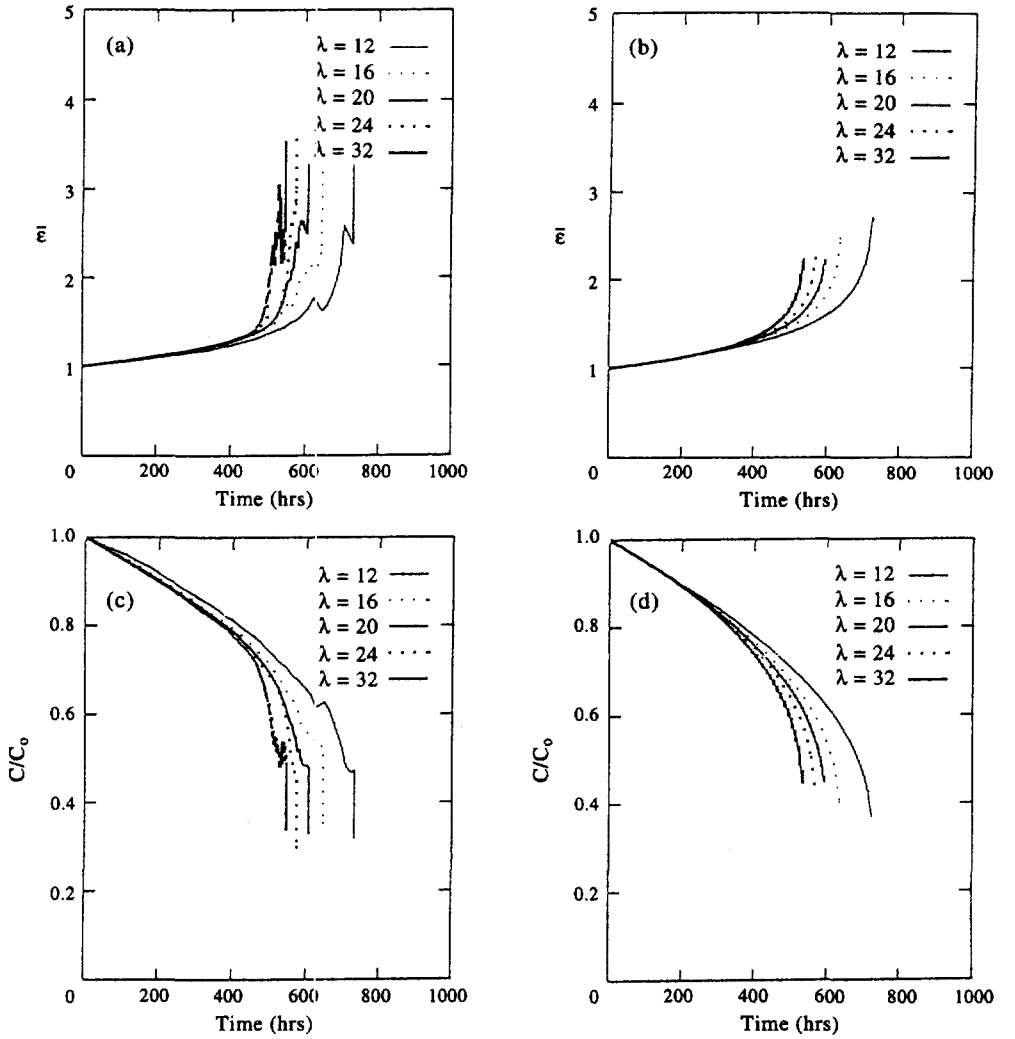

Fig. 9. Creep strain plotted vs time (a) simulations and (b) analytical model, and effective lattice stiffness plotted vs time (c) simulations and (d) analytical model.

without regard to the circumstances, selection of the damage parameter and damage mode. A proper local micromechanical damage model provides a relation between the microcrack density and effective transport properties of the solid assuming it to be statistically homogeneous or self-similar (Krajcinovic and Mastilovic, 1995). Thus, if the onset of a transition (bifurcation) to a state of failure can be predicted from the effective transport properties of the thermodynamic state at the incipient failure it logically follows that the onset of this failure *can* be defined in terms of the critical value of the micromechanically correct damage parameter as well.

Unstable growth of a single Griffith's crack is a typical example of a brittle failure that has little in common to the distributed damage and/or damage mechanics. Damage mechanics is applicable to the case of a stable evolution of microcracks. This study summarizes and compares three different failure modes characterized by the damage evolution that is, prior to the failure, stable and dominated by random nucleation of defects. The loss of homogeneity is attributed to the increase of the defect cluster size $\xi \to L$ that is common to the three considered failure modes. The difference between these modes is related to the mechanism that drive the cluster growth and the rate of the cluster growth.

In the case of strain localization the growth of the defect cluster (fault) is attributed to the interaction of cooperative effect. The energy release rate G is distributed along the band perimeter. The local, mean field damage models (that do not account for the defect

interaction) cannot be expected to provide a very accurate prediction of the localization onset which depends on the local stresses amplified by the crack interaction. After the loss of homogeneity on the specimen scale the fault grows very rapidly and the softening part of the force-contraction curve is very steep. This reduces the problem of the prediction of the localization onset to the determination of the force and displacement at the peak of the curve. Assuming the curve to be C_1 continuous at the peak a proper micromechanical damage mechanics model should suffice to provide a reasonably good estimate of the localization onset [see Krajcinovic (1996) for a related problem].

The mean field micromechanical estimates of the percolation threshold, at which the cluster of cracks transects the specimen, are notoriously accurate. This should be expected since the condition (2) is never violated due to the fact that the damage evolution is not dependent on stresses, defect interaction and stress distributions. The morphology of the defect clusters is gossamer-like. Naturally, mean-field models fail to describe accurately the states near the percolation threshold.

The creep rupture mode depends on the temperature and stresses. When the temperature dominates the damage evolution process is random preserving the material homogeneity until imminent rupture. Defect clusters are in shape similar to those characterizing the percolation. Simple damage models are quite accurate for the determination of time to rupture. Somewhat more involved damage models are necessary to model the tertiary creep phase. The accuracy degenerates at larger tensile stresses. Defect clusters are tighter and the stress concentrations (extreme statistics of stress distribution) large enough to become the dominant force that drives the damage evolution.

In summary, the qualitative studies in this paper indicate that rather simple, local damage micromechanical models may, under considered circumstances, provide accurate estimates of failure onsets. All considered cases are characterized by the absence of the long range tensile stresses. Since the utilization of materials with inferior tensile strengths, susceptible to brittle deformation, is in design limited to structures in which the long range tensile stresses are absent the role of damage mechanics in estimating the onset of failure is after all, more substantial than was originally suspected.

Acknowledgement—The authors gratefully acknowledge the financial support in the form of a research grant from the U.S. Department of Energy, Office of Basic Energy Research, Division of Engineering and Geosciences to the Arizona State University, which made this work possible.

REFERENCES

Bazant, Z. P. and Cedolin, L. (1991) *Stability of Structures, Elastic, Inelastic, Fracture and Damage Theories*. Oxford University Press, New York.

Benguigui, L. (1984) Experimental study of the elastic properties of a percolating system. *Physics Review Letters* **53**, 2028–2030.

Cai, Y. and Thorpe, M. F. (1989) Floppy modes in network glasses. *Physics Review B* **40**, 10,535–10,542.

Eyring, H. (1936) Viscosity, plasticity and diffusion as examples of absolute reaction rates. *Journal of Chemistry and Physics* **4**, 283–291.

Garboczi, E. J. and Thorpe, M. F. (1985) Effective-medium theory on central-force networks. II. Further results. *Physics Review B* **31**, 7276–7281.

Gaudett, M. A. and Scully, J. R. (1994) Application of bond percolation theory to intergranular stress-corrosion cracking of sensitized AISI 304 stainless steel. *Metallurgy and Material Transactions A* **25A**, 775–787.

Hallbauer, D. K., Wagner, H. and Cook, N.G.W. (1973) Some observations concerning the microscopic and mechanical behavior of quartzite specimens in stiff, triaxial compression tests. *International Journal of Rock, Mechanics, Mineral Science and Geomechanical Abstracts* **10**, 713–726.

Hansen, A. and Roux, S. (1988) Multifractality in elastic percolation. *Journal of Statistical Physics* **53**, 759–771.

Hansen, A. and Roux, S. (1991) Scale-invariant disorder in fracture and related breakdown phenomena. *Physics Review B* **43**, 665–678.

Horii, H. and Sahasakmontri, K. (1990) Mechanical properties of cracked solids. In: *Micromechanics and Inhomogeneity*, eds. G. Weng, M. Taya and H. Abe. Springer, New York, pp. 137–159.

Hult, J. (1974) Creep in continua and structures. In: *Topics in Applied Mechanics*, eds. J. L. Zeman and F. Ziegler. Springer, Wien, Austria, pp. 137–155.

Jasiuk, I., Chen, J. and Thorpe, M. F. (1994) Elastic moduli of two-dimensional material with polygonal and elliptical holes. *Applied Mechanics Review* **47**, S18–S28.

Ju, J. W. and Tseng, K. H. (1995) An improved two-dimensional micromechanical theory for brittle solids with randomly located microcracks. *International Journal of Damage Mechanics* **3**, 23–57.

Krajcinovic, D. (1996) *Damage Mechanics*. North-Holland, Amsterdam.

Krajcinovic, D. and Mallick, K. (1995) Micromechanics of the process induced damage in thermosets. *Journal of Mechanics and Physics of Solids* **43,** 1059–1086.

Krajcinovic, D., Mallick, K., Basista, M. and Sumarac, D. (1992a) Elastic moduli of perforated plates in the neighborhood of critical state. *International Journal of Solids and Structures* **29,** 1837–1847.

Krajcinovic, D. and Mastilovic, S. (1995) Some fundamental issues of damage mechanics. *Mechanics Materials* **21,** 217–230.

Krajcinovic, D., Sumarac, D. and Mallick, K. (1992b) Elastic parameters of brittle, elastic solids containing slits. *International Journal of Damage Mechanics* **1,** 386–403.

Krajcinovic, D. and Vujosevic, M. (1998) Strain localization—short to long correlation-length transition. *International Journal of Solids and Structures*, in press.

Krausz, A. S. and Krausz, K. (1988) *Fractures Kinetics of Crack Growth.* Kluwer, Dordrecht, The Netherlands.

Lawn, B. R. (1993) *Fracture of Solids*, 3rd edn. Cambridge University Press, Cambridge, U.K.

Lemaitre, J. (1992) *A Course on Damage Mechanics.* Springer, Berlin.

Lockner, D. A., Moore, D. E. and Reches, Z. (1992) Microcrack interaction leading to shear fracture. In: *Rock Mechanics*, eds. J. R. Tillerson and W. R. Wawersik. Balkema, Rotterdam, The Netherlands, pp. 807–816.

Mastilovic, S., Vujosevic, M. and Krajcinovic, D. (1996) Localization in disordered brittle media: lattice models. In: *Advances in Failure Mechanics in Brittle Materials*, eds. R. J. Clifton and H. D. Espinoza. ASME, MD-Vol. 75, AMD-Vol. 219, pp. 171–184.

Mura, T. (1982) *Micromechanics of Defects in Solids.* M. Nijhoff, The Hague, The Netherlands.

Nemat-Nasser, S. and Hori, M. (1993) *Micromechanics: Overall Properties of Heterogeneous Materials.* North-Holland, Amsterdam.

Ostoja-Starzewski, M. (1994) Micromechanics as a basis of continuum random fields. *Applied Mechanics Review* **47,** S221–S230.

Paterson, M. S. (1978) *Experimental Rock Deformation—the Brittle Field.* Springer, Berlin.

Popper, K. P. (1992) *The Logic of Scientific Discovery.* Routledge, New York.

Reches, Z. and Lockner, D. A. (1994) Nucleation and growth of faults in brittle rocks. *Journal of Geophysics Research* **99,** 18,159–18,173.

Regel' V. L., Slutsker, A. I. and Tornashevski, E. E. (1974) *Kinetic Theory of Strength of Solids.* Nauka, Moscow (in Russian).

Rice, J. R. (1976) The localization of plastic deformation. In: *Proceedings of the 14th International Congress of Theoretical and Applied Mechanics*, ed. W. T. Koiter. North-Holland, pp. 207–220.

Riedel, H. (1987) *Fracture at High Temperatures.* Springer, Berlin.

Roux, S. and Hansen, A. (1990) Early stages of rupture of disordered materials. *Europhysics Letters* **11,** 37–42.

Rudnicki, J. W. and Rice, J. R. (1975) Conditions for localization of deformation in pressure-sensitive dilatant materials. *Journal of Mechanics and Physics of Solids* **23,** 371–394.

Sieradzki, K. and Li, R. (1986) Fracture behavior of solids with random porosity. *Physics Review Letters* **56,** 2509–2511.

Sofo, J., Lorenzana, J. and Martinez, E. N. (1987) Critical behavior of Young's modulus for two-dimensional randomly holed metalized mylar. *Physics Review B* **36,** 3960–3962.

Sornette, A., Davy, P. and Sornette, D. (1990) Growth of fractal fault patterns. *Physics Review Letters* **65,** 2266–2269.

Stauffer, D. and Aharoni, A. (1992) *Introduction to Percolation Theory*, 2nd edn. Taylor and Francis, Washington, DC.

Termonia, Y., Meakin, P. and Smith, P. (1986) Theoretical study of the influence of strain rate and temperature on the maximum strength of perfectly ordered and oriented polyethylene. *Macromolecules* **19,** 154–159.

Vardoulakis, I. and Graff, B. (1985) Calibration of constitutive models for granular materials using data from biaxial experiments. *Geotechnique* **35,** 299–317.

Vujosevic, M. and Krajcinovic, D. (1997) Creep rupture of polymers—a statistical model. *International Journal of Solids and Structures* **34,** 1105–1122.

Xia, W. and Thorpe, M. F. (1988) Percolation properties of random ellipses. *Physics Review A* **38,** 2650–2656.